

ORIGINAL RESEARCH

LW-CovidNet: Automatic covid-19 lung infection detection from chest X-ray images

Noor Ahmed  | Xin Tan | Lizhuang Ma

School of Electronic Information and Electrical Engineering, Department of Computer Science and Engineering, Shanghai Jiao Tong University, Shanghai, China

Correspondence

Noor Ahmed, School of Electronic Information and Electrical Engineering, Building-3, Room 507-3, 800, Dongchuan road Minhang campus, Shanghai 200240, China.

Email: noorahmedakbar2016@yahoo.com

Lizhuang Ma, School of Electronic Information and Electrical Engineering, Dongchuan road Minhang campus, Shanghai 200240, East China Normal University, 200062, China.

Email: ma-lz@cs.sjtu.edu.cn

Funding information

Shanghai Municipal Science, Technology Major Project, Grant/Award Number: 2021SHZDZX0102; Shanghai Jiao Tong University, Grant/Award Number: ZH2018ZDA25; Shanghai Science and Technology Commission, Grant/Award Number: 21511101200

Abstract

Coronavirus Disease 2019 (Covid-19) overtook the worldwide in early 2020, placing the world's health in threat. Automated lung infection detection using Chest X-ray images has a ton of potential for enhancing the traditional covid-19 treatment strategy. However, there are several challenges to detect infected regions from Chest X-ray images, including significant variance in infected features similar spatial characteristics, multi-scale variations in texture shapes and sizes of infected regions. Moreover, high parameters with transfer learning are also a constraints to deploy deep convolutional neural network(CNN) models in real time environment. A novel covid-19 lightweight CNN(LW-CovidNet) method is proposed to automatically detect covid-19 infected regions from Chest X-ray images to address these challenges. In our proposed hybrid method of integrating Standard and Depth-wise Separable convolutions are used to aggregate the high level features and also compensate the information loss by increasing the Receptive Field of the model. The detection boundaries of disease regions representations are then enhanced via an Edge-Attention method by applying heatmaps for accurate detection of disease regions. Extensive experiments indicate that the proposed LW-CovidNet surpasses most cutting-edge detection methods and also contributes to the advancement of state-of-the-art performance. It is envisaged that with reliable accuracy, this method can be introduced for clinical practices in the future.

1 | INTRODUCTION

The rapid spread of corona virus disease has sparked worldwide fear since December 2019. Currently, real-time polymerase chain reaction (RT-PCR) detection of viral nucleic acids is one of the acceptable and viable standard clinical covid-19 detection tool. [1, 2]. The covid-19 pandemic is rapidly intensifying, with hundreds of fatalities and thousands of infections occurring every day in various places, posing significant problems in combating the virus. Many hyper-endemic regions or countries are unable to deliver appropriate RT-PCR testing to tens of thousands of suspected patients. These methods are exceedingly lengthy and tedious, regardless of whether they are readily accessible in all epidemic regions. However, it is a lengthy procedure with a high number of false negatives. [3]. In addition, numerous studies have shown that most of the conventional methods of detecting diseases are ineffective [4, 5] leading to an

ineffective and unsuitable treatment for the patients. It is imperative to develop an AI-based deep-learning system for the detection of covid-19 that is automated and cost-effective. Furthermore, the following are the key concerns that act as limits on existing automated systems.

(a) The large number of learning parameters are constraints to implement deep learning models in real time applications. (b) The most of the work done in the realm of covid-19 detection [6–9] are based on transfer learning due to unavailability of large number of dataset.

However transfer learning requires a lot of manual efforts due to compatibility issues of transfer learning method with unseen datasets, detection accuracy can be compromised. However disease detection process demand a high accuracy. (c) covid-19 infection detection Chest X-ray images is a challenging task, owing several issues: i.e. similar spatial characteristics, multi-scale variations in texture shapes and sizes of infected regions

This is an open access article under the terms of the [Creative Commons Attribution-NonCommercial-NoDerivs](https://creativecommons.org/licenses/by-nc-nd/4.0/) License, which permits use and distribution in any medium, provided the original work is properly cited, the use is non-commercial and no modifications or adaptations are made.

© 2022 The Authors. *IET Image Processing* published by John Wiley & Sons Ltd on behalf of The Institution of Engineering and Technology

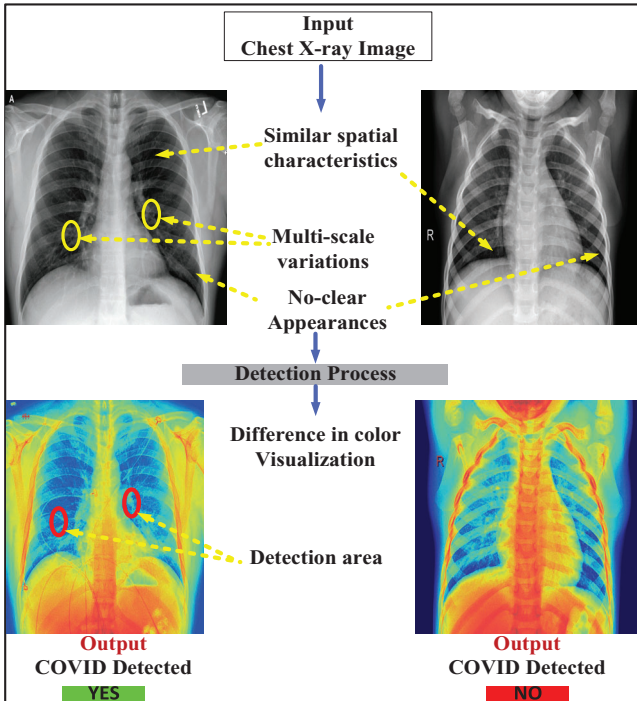


FIGURE 1 Normal Chest X-ray image(right). Covid-19 Chest X-ray (left). The pathogenic structure i-e similar spatial characteristics, multi-scale variations in texture shapes and sizes of infected regions in the left Chest X-ray image cannot be easily distinguished from the right Chest X-ray image

are obvious issues in finding the infected area from Chest X-ray images. For example, infected disease regions are varying as small and large sizes, this easily leads to the detection of false-negatives during inference time. For example, Figure 1 shows infected areas often have no clear appearances from uninfected areas and it is very difficult for doctor's and machine's to distinguish normal image from infected image in proper and also effects in making doctor's and machine decision process to detect covid-19.

In this context to address above-mentioned issues, we propose a new method to detect covid infectious regions based on integrating Standard and Depth-wise Separable convolutions with an Edge Attention Block. This new method can detect covid-19 cases accurately in the presence of aforementioned occlusion challenges. The method was motivated by the urgent need for a solution to fight against the covid-19 pandemic, inspired by the scientific community's open source access efforts, and attentive of AI-based methods' efficacy. Extensive experimentation on datasets, such as COVID-19 Lungs[10], COVID-CT[11], COVID-19[12], COVID-19-Radiography[13, 14], confirm the proposed method's effectiveness in generalization.

The main contributions proposed in this study are based on three main factors: (1) For early detection of covid-19, a new architecture based on Standard and Depth-wise Separable convolution neural network is proposed. (2) A novel method is used to expand the Receptive Field of the model for better detection of infected regions in the presence of detection challenges. (3) The proposed method achieves the state-of-the-art

performance under varying detection challenges such as similar spatial characteristics, multi-scale variations in texture shapes and sizes of infected regions.

The study is structured as follows: Section 2 underlines the relevant work that has already been done; Section 3 stresses upon the different materials and methods used in this study; Section 4 recollects on the limitations demonstrated by the already present state-of-the-art methods; Section 5 exhibits the contributions of the present work; Section 6 demonstrates the experimental work and discussion of the obtained results; Section 7 discusses the limitations of the proposed method, whereas Section 8 is a summary of the overall findings from this study.

2 | RELATED WORK

Deep learning methods have recently been devised to detect covid-19 affected patients using radiological imaging [15, 16]. Like, Wang et al. [17] proposed a method based on lightweight architecture with accuracy and sensitivity of 93.3% and 91.0%, respectively, to detect covid-19 cases from Chest radiography images. The method uses 1×1 convolutions to expand features into higher dimensionality and extends channel dimensionality for the final output. Sarker et al. [18] used Densenet-121 model with a transfer learning method and achieved 92.91% accuracy for two-class and three-class, classifications. Furthermore, Ozturk et al. [19] developed a 17 layer's of convolutional model based on DarkNet that obtained binary and multi-classification accuracy of 98.8% and 81.02%, respectively. Bassi et al.[20] proposed a deep transfer learning on basis of Imagenet pretrained method to classify Chest X-ray images. To detect covid-19 patient's cases from Chest X-ray images, Al-Rakhami et al.[21] also used a transfer learning strategy that included VGG19, DenseNet121, InceptionV3, and Inception ResNetV2. Mahmud et al.[22] proposed a multi-dilation CNN with a transferable multi-receptive feature optimization method for the detection of covid-19 cases. Minaee et al.[23] used a deep transfer learning architecture to identify infected regions from other lung diseases, employing 71 covid-19 samples. To detect coronavirus cases, the proposed deep design transfer learning method had an overall sensitivity of 97.5% and specificity of 90%. Rahimzadeh et al.[24] devised a concatenated Xception and ResNet50V2 network. The network was trained across eight phases with a total of 633 data, including 180 covid-19 samples in each step. Apostolopouloset et al.[7] proposed another transfer learning method for the detecting of coronavirus infection, with accuracy 93.48%, specificity of 92.85% with sensitivity of 98.75% the VGG19 outperformed the other competitors. Horry et al.[25] revealed that a deep transfer learning-based system surpassed the competitors of VGG19 with an 83% sensitivity and precision for covid-19 detection. To detect coronavirus-infected patients, Kumar et al.[26] proposed a transfer learning-based system that included pre-trained CNNs and a support vector machine, using three pre-trained CNN networks, ResNet50-SVM outperformed the other models with an accuracy of 95.38%. Another deep transfer learning

method proposed by Loey et al.[27], this study used 69 covid-19 samples, 79 pneumonia bacterial samples, 79 pneumonia viral samples, and 79 normal samples. In the four-case scenario, GoogleNet has an average accuracy of 80.6% in the four-case scenario. Bukhari et al.[28] have proposed a transfer learning methodology. The method was tested on 89 covid-19 samples and had 98.18% accuracy.

The literature review reveals that the current state-of-the-arts methods mostly utilized transfer learning based methods with large number of parameters. For transfer learning the training data must have two possibilities. To begin, the pre-trained model's training data distribution must be similar to the data that will be seen during test time, or at the very least not differ too much. Second, the number of training data for transfer learning should be appropriate to avoid overfitting the model. When someone transfers the data content from an ordinary type to a medical domain, such as detection of covid-19 patients under challenging circumstances such as shape, size, and other variation of infected regions, transfer learning may have a very limited effect. Our motivation is driven by the fact that, transfer learning may not be better than scratch training in the domain of detecting covid-19 cases, as the networks learn quite different high-level features depending on the task.[29].

However covid-19 detection process demands a high accuracy and minimum parameters for real time applications in the presence of challenges like similar spatial characteristics, multi-scale variations in shape and sizes of infected regions. These deficiencies have been addressed by a new proposed method.

3 | MATERIALS AND METHODS

3.1 | Data preprocessing and augmentation

We have collected data from all over the world from diverse open sources in order to train the proposed model in a well generalized manner. The initial Covid-19 Lungs[10] dataset includes X-ray images of patients who have been infected with covid-19, SARS, Streptococcus, ARDS, Pneumocystis, and other strains of pneumonia. There were 98 Chest X-ray images from 70 covid-19 patients and 28 normal Chest X-ray images in this study. The second dataset COVID-CT[11] has 1288 cases, including 288 covid-19 patient and 1000 normal cases. The third dataset[12] is comprised of X-ray images comprising 229 covid cases and 0 normal cases. Due to lack of covid-19 cases inside mentioned datasets. The method used another dataset such as COVID-19-Radiography[13, 14] contains X-ray images with 219 covid-19 cases and 2686 normal cases orderly to balance the covid-19 cases with normal cases. We have combined these datasets as a single dataset containing total of 4520 images and named as covid-19 dataset, all details are listed in Table 1. The implementation of proposed method was initiated by converting the size of all dataset images to 224×224 . The dataset images are enhanced by augmentation technique to remove any overfitting to achieve better accuracy when the test is initiated. The enhancement of these images involves a horizontal and vertical flipping giving 20-degree affine image rotation and 0.1

probability rate. The method of width and height shift-range of 0.1, and a shear range of 0.05, a re-scale range of $1/255.0$ and a zoom range of 0.05, all are included in augmentation. The proposed method assures that these augmentations will not cause any discrepancies in the original structure of the datasets while keeping them authentic.

4 | PRELIMINARIES

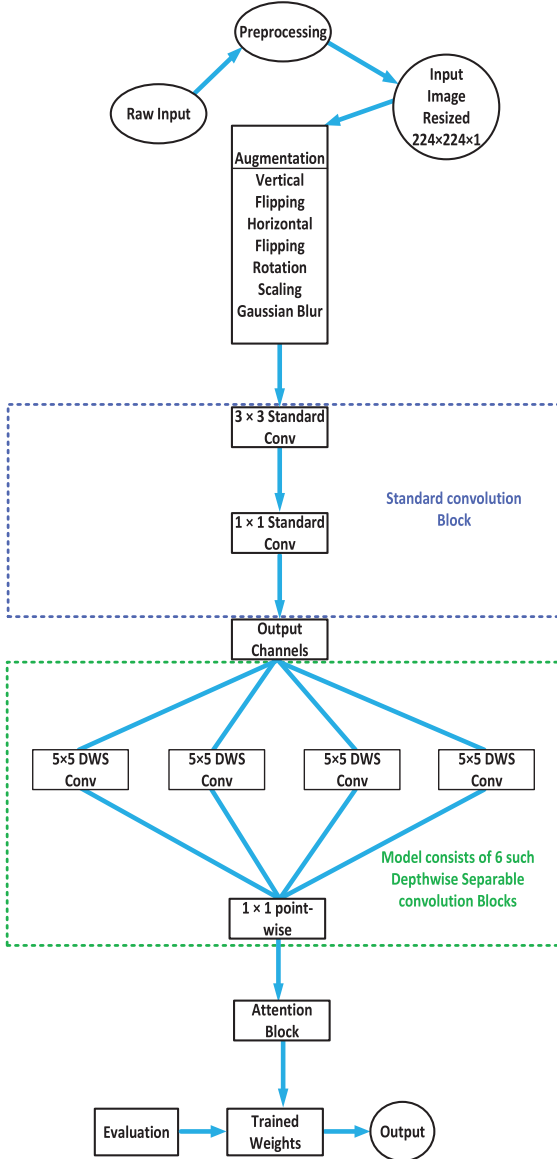
The majority of the state-of-the-art model's architectures, including LeNet [30], AlexNet [31], VGG Net [32] use a stack of convolutional layers followed by pooling layers. The extracted features from these layers are further enhanced for the purpose of detection at Fully Connected layers(FC) and then softmax or sigmoid layers are used at the end for class level prediction. Significant developments in architectures, such as DenseNet [33], FractalNet [34], GoogLeNet [35], and Residual Networks [36] are evident in the past few years to further enhance detection. Numerous object recognition and detection tasks have been accurately performed with the help of these architectures, such aspects increase the importance of these architectures. However all of these model's architectures observe the same basic structure of utilizing convolution and pooling layers such as max-pooling, average pooling and FC layer. However differences can observe in the modern deep learning architectures[37]. The number of parameters are high by using Standard CNN with FC layers or dense layers. The results are negatively affected by the utilization of max and average pooling, however such traditional methods of using pooling layers would lose a lot of image features and a FC would dramatically increase the number of parameters, forcing network training to take more time[38]. The proposed method network's architecture eliminates the utilization of pooling layers and distinct FC layers owing such deficiencies, however large number of parameters are also constraints in implementation of CNN models specifically with transfer learning method in real time applications. Furthermore, various oscillations and multi-scale class variations challenges in medical datasets make it challenging to detect infected regions using traditional pooling methods i-e average and max pooling [39, 40]

5 | PROPOSED METHOD

The section provides an overview of the proposed method as well as details on how it works. The propose method extract important features from training images dataset for making disease analysis efficient. The proposed method's model is trained using covid-19 infected Chest X-ray images as well as normal images of collected datasets form different sources[10–14]. The trained model is then evaluated over the validation images of covid-19 dataset. The trained weights then unveil the disease regions from Chest X-ray images during the network inference time and also applies heatmaps for accurate boundary detection of each regions. Figure 2 depicts a high-level overview of the proposed method.

TABLE 1 Covid-19 Imaging datasets that are publicly available. The number of covid-19 and Non-covid cases are denoted by covid-19 and normal, respectively

Dataset	Nature of images	Covid-19/normal	Task
COVID-19 Lungs[10]	X-rays	70/28	Detection
COVID-CT[11]	Computed Tomography(CT) Images	288/1000	Detection
COVID-19[12]	X-rays	229/0	Detection
COVID-19-Radiography[13, 14]	X-rays	219/2686	Detection

**FIGURE 2** Flow-chart of the Proposed LW-CovidNet

5.1 | Network overview

The paper proposes a well-generalized Lightweight Convolutional Neural Network based on scratch learning (SL). The proposed method incorporates, Standard as well as Depth-wise Separable convolutions with skip connections. To enhance the

detection capability of the network, it has also been embedded with an Edge Attention Block, Figure 3. There are two Standard convolutional layers in the first block of model with convolutional layers of sizes 3×3 and 1×1 . It uses a dilation rate of 6, a kernel regularizer of 0.01 and a bias regularizer of 0.01. A batch normalization and non-linear activation function like Relu is used in first block of the model to restrain the quantity of parameters as well as, at the same time, strengthen the network to provide a brief depiction of the input image. The next to the Standard convolution block there are six consecutive Depth-wise Separable blocks. These blocks have parameters like depth multiplier =6 and dilation-rate =6, respectively. Next to the consecutive six blocks of Depth-wise separable convolutional layers, the sequence now continues with a block of an Edge Attention. A practical application of Dropout 0.25 [41] is applied to avoid overfitting after blocks 4, 5 and 6. The traditional method of utilization average or max-pooling layers have not been used due to their characteristic of decreasing the spatial dimension, however 1×1 convolutions are used in all blocks for the purpose of channel dimensionality reduction. Relu is used inside the whole method after each block as mentioned in Figure 3. The padding within the Standard convolutional block and Depth-wise Separable convolutions blocks used as “same”, whereas the depth-multiplier rate is recorded as 6 in the first block of Standard convolution. The final phase of the architecture consists of a k-way sigmoid activation in generating distributions over k class labels at Edge Attention block to decide that the final prediction is covid 19 infected or normal region. Algorithm 1 depicts the proposed method’s whole procedure of working. The Network’s additional details are as follows:

5.2 | Edge attention block

Traditional methods use FC layers to determine decision boundaries for class categories, whereas increasing model parameters at the same time causes overfitting based on the network model’s complexity.[42]. Conversely, Global Average Pooling (GAP) is a method through which the feature map in the previous layers can be assessed through an average output. The FC layers are usually replaced by GAP as it matches the target classes while producing the feature map for final prediction[43]. GAP is merely an operation used for the final classification to prepare the model and does not apply any parameters while eliminating the chances of overfitting.

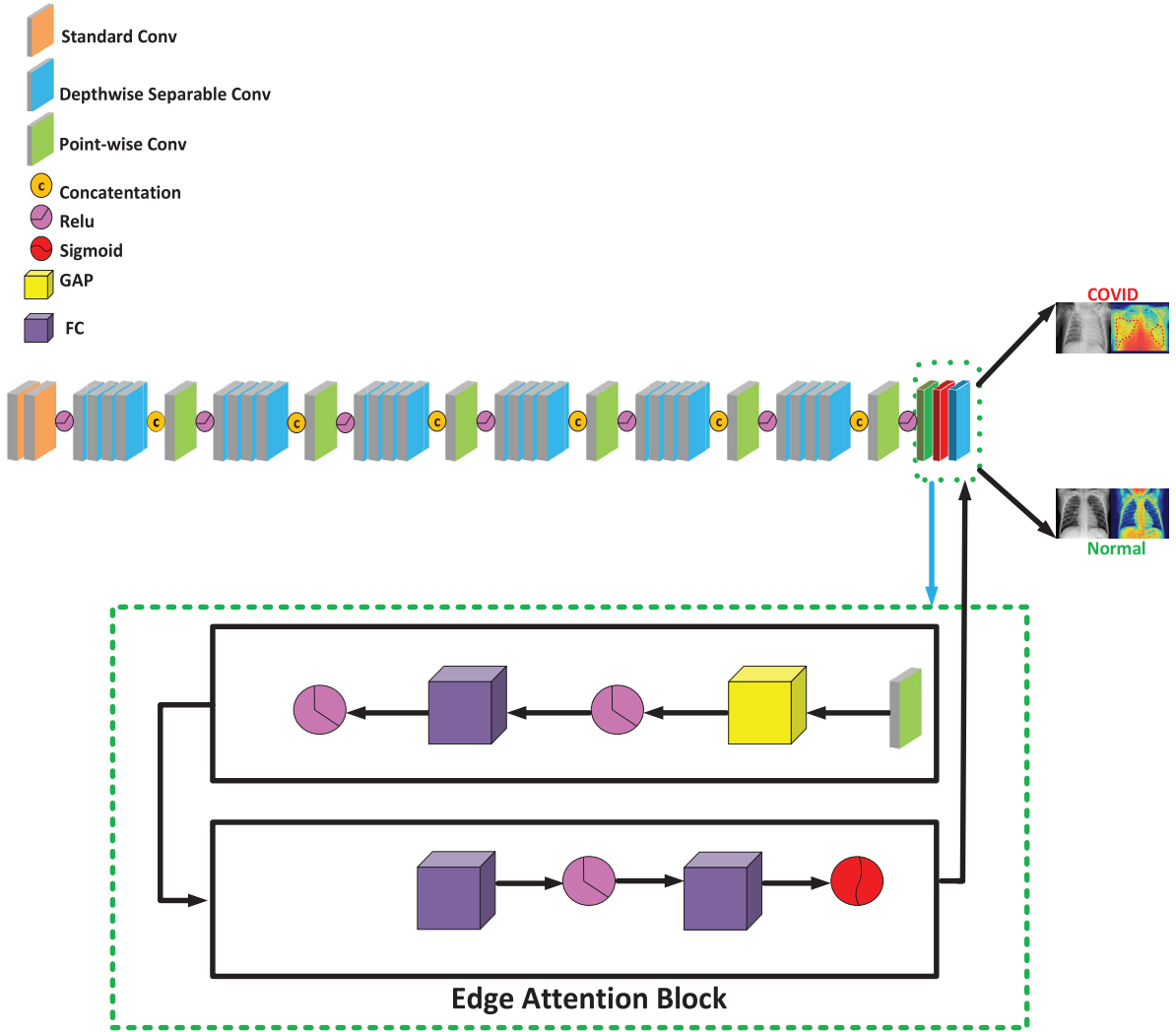


FIGURE 3 Experimental figure of the proposed network architecture using Standard and Depth-wise Separable convolutions layers with an Edge Attention Block

A method proposed in this study, known as the hybrid weight method, increases the analytical capacity of the network model while integrating the two blocks; like first module composed of 1×1 point-wise convolution connected with GAP and FC modules via ReLU non-linear activation functions. Furthermore the second module of Edge Attention Block composed of two FC modules connected together via a ReLU and finally combined through a sigmoid layer as whole process is shown at Edge Attention Block of Figure 3. As a result, deep convolutional models can easily experience a decrease in the number of integrated parameters. Edge Attention Block, categorizes the features into covid and normal images by applying distinct color heatmap. Let us suppose the $\alpha(x, y)$ represents the weight at spatial location (x, y) of an input image $x(m, n)$, formerly $S_c(x, y)$ represents the prediction of class k , i-e $k = 2$ classes which is computed in Equation (1).

$$S_c = \sum_{x,y} \alpha(x,y) S_c(x,y). \quad (1)$$

To aggregate features, disease region prediction is given as

$$S_c = \sum_k \omega_k^c \sum_{x,y} \alpha(x,y) f_k(x,y), \quad (2)$$

where ω_k^c is the hybrid classification weight correspond to class k and $f_k(x,y)$ represents the activation of class unit k , when $S_c(x,y) = \sum_k \omega_k^c f_k(x,y)$ from Equations (1) and (2).

It is vital that the weight $\alpha(x,y)$ [44] in the given method must fulfill the following rules: Most importantly, the weight should not have a negative value, that is, $\alpha(x,y) \leq 0$ and $\sum_{x,y} \alpha(x,y) \neq 0$. In reality, a higher weight can contribute more performance gains to the results than a lower weight. According to this, the weight has to be near to 1 or $\sum_{x,y} \alpha(x,y) = 1$. With such attributes, the Edge Attention Block aggregate features with high weight and surpass low weights. Hence, weight $\alpha(x,y)$ strengthens the network to efficiently identify the boundary regions of infected regions from Chest X-ray images.

ALGORITHM 1 The main Framework of LW-CovidNet

- 1: Preprocessed: resized images to 224×224
- 2: Feature extraction from input image by using 3×3 conv layer
- 3: The Standard convolution 1×1 layer performed as channel-wise pooling for dimensionality reduction
- 4: layers.add(ReLu)
- 5: layers.add(batch_normalization)
- 6: layers.add(Depth-wise separable convolution 5×5) each block contain 4 such layers
- 7: Concatenate: Depth-wise Separable convolution to increase Receptive Field to gain deep features form input image
- 8: Apply:point-wise separable convolutions(1×1 point-wise) to combine the features by channel wise operation from layer 1 to 4
- 9: Repeat: The process repeats the same procedure in 6 blocks until for better recognition of features
- 10: layers.add(1×1 point-wise)
- 11: layers.add(GAP)
- 12: layers.add(ReLu)
- 13: layers.add(FC)
- 14: layers.add(ReLu)
- 15: layers.add(FC)
- 16: layers.add(ReLu)
- 17: layers.add(FC)
- 18: layers.add(sigmoid)
- 19: return layers

5.3 | Standard and depth-wise separable convolutions

This section consists of a comparison between Standard Convolutions [36] and Depth-wise separable (DWS) convolutions [45, 46]. A number of effective architectures [45–48] have used convolution factorization as a fundamental element. The Standard convolution is replaced by a resolved version of the convolution, such as a Depth-wise separable convolution. A Depth-wise convolution takes an input $X \in \mathbb{R}^{W \times H \times C}$ by using a convolutional kernel $K \in \mathbb{R}^{n \times n \times c}$ to produce an output $Y \in \mathbb{R}^{W \times H \times C}$ by learning parameters $n^2 \hat{c} + \hat{c}$ from an effective Receptive Field. The computation cost can be decreased through this characterization.

In contrast, LW-CovidNet decreases the computational burden, as it decomposes Standard convolution in the model's first block and then applies Depth-wise Separable convolution with point-wise convolutions from second to sixth block. It happens in two steps; (1) The first step involves applying a Standard convolution n of size 3×3 and 1×1 with a dilation rate r of 6, (2). A point-wise convolution layer n of size 1×1 is applied at the end of each block to reduce the channel depth as shown in Figure 3. Furthermore, Figure 4d represents the proposed model layers with Standard Depth-wise Separable convolutions including point-wise convolutions. These layers are formed when the Depth-wise Separable convolutions utilize light weight filtering instead of a Standard convolution. The outputs produced by the

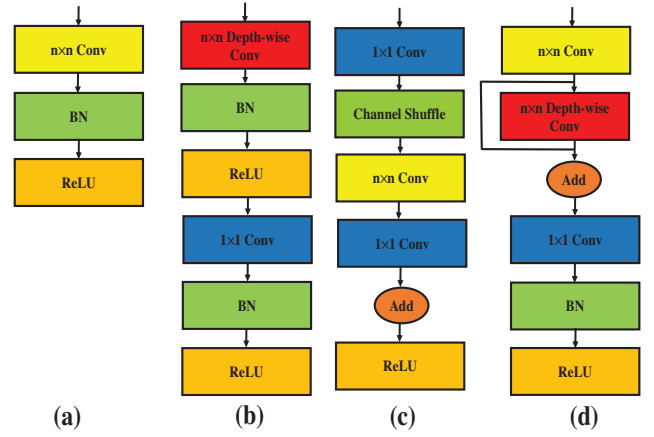


FIGURE 4 Structural view of Standard and Depth-wise Separable convolutions in state-of-the-art methods and proposed method. (a) Standard convolution; (b) MobileNet; (c) ShuffleNet; (d) Proposed Model

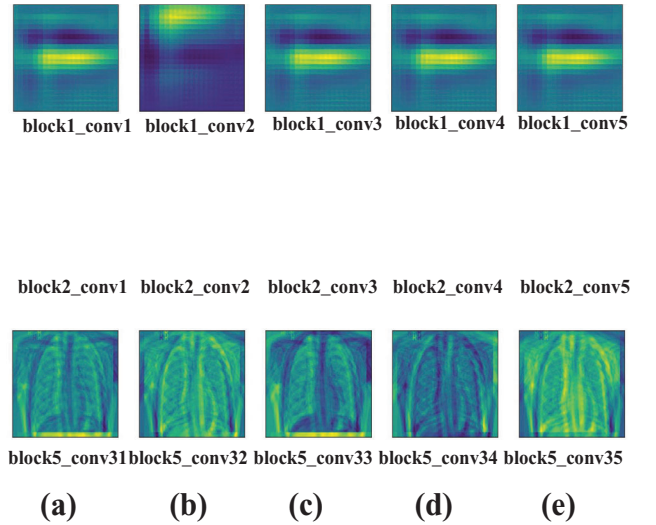


FIGURE 5 The above images show how the Network's Receptive Field affects various features extracted from the input image by successive layers of LW-CovidNet; the first levels relate to low-level features like edges, while the later layers show high-level features like white filtrates. etc.

Depth-wise layer are then used by the point-wise convolution to create a linear combination utilizing a convolution stated as 1×1 . The efficiency of the convolution network is maximized by the ability of point-wise convolution to retain spatial information. Moreover, there are four such Depth-wise Separable convolutions layers with in each block of Depth-wise Separable convolutions as applied in this method. These convolutions are in the form of six blocks, where $n = 5$ Figure 6c. Moving on, the method applies a n of size 1×1 point-wise convolution after combining the output of the previous step's block. A decrease in model parameters from $n^2 \hat{c}$ to $1/n + \hat{c}$ occurs through such characterization in the process. Several observations can be made from Table 2, including the contrast between various convolutions, parameters and Receptive Field.

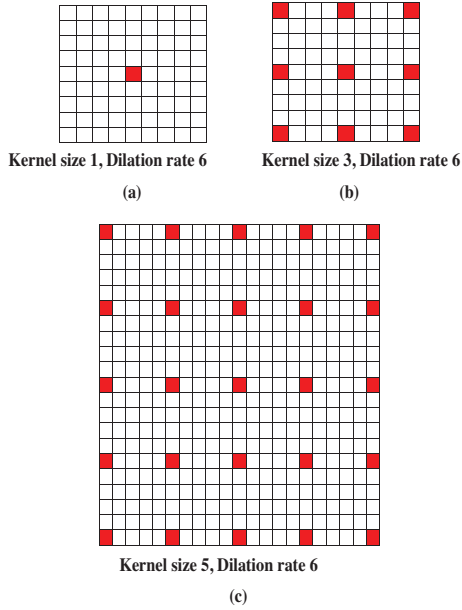


FIGURE 6 Convolutional kernels of sizes of 1×1 , 3×3 , 5×5 with dilation rate of 6

TABLE 2 Comparison between different types of convolutions. Here $n_r = (n - 1)$. $r + 1$ represents dilation rate. “DW” represents Depth-wise Separable convolution

Convolutions	Parameters	Size of receptive field
Standard[36]	$n^2 \hat{c}$	$n \times n$
DW [45]-[46]	$n^2 \hat{c} + \hat{c}$	$n \times n$
LW-CovidNet	$1/n + \hat{c}$	$(n + 1) \times (n + 1)$

5.4 | Method of improving receptive field

Receptive Field has great significance in gaining plenty of information from low resolution, images for performing a visual task. However, for other fields of the domain, a Receptive Field of Standard convolution of size 3×3 kernel is enough. To extract enough information from medical images with low contrast and many variations of disease regions need an increased Receptive Field with a proper feature extraction method[49]. In general, the Receptive Field contains both image input values in the spatial domain and channel dimensions[50]. However, in our proposed work, we focused on the spatial dimensions within a convolutional layer. Spatial Receptive Field is defined by the kernel size of the previous layer; the higher the kernel, the more activation it can observe. In general, increasing the depth of the model by stacking more and more convolution layers, increasing the kernel sizes of convolutional layers, stride rate, and using greater dilation rate or continuous variations in dilation rate such all procedures increase Receptive Field. However, Such methods increase the complexity of network by increasing computational cost in the form of increasing parameters. Furthermore, the proposed method compensates

for this deficiency by utilizing a constant Depth-wise separable convolutional of kernel size (5×5) , constant dilation rate of 6, and Depth-wise multiplier of 6 in each block of Depth-wise Separable convolutions and merging these kernels with a point wise convolution size of (1×1) . The comparative effect of Receptive Field on input images along spatial dimension, can be visualized in Figure 5a–e. As color density in the input image increases, the relationship between both Receptive Field and feature maps increases.

The maximum Receptive Field size can be calculated using the following equation[50].

$$S_n = S_{n-1} * s_n$$

$$RF_n = RF_{n-1} + (k_n - 1) * S_n, \quad (3)$$

where s_n, k_n are stride and kernel size of layer n , respectively. S_n, RF_n are commutative stride Receptive Field RF from layer n of the network.

5.5 | Comparison with light weight methods

The method is compared with other light weight models, including MobileNet V2 [46], ESPNet V2 [51], ShuffleNet v2 [45], SqueezeNet V2 [52], and COVID-Net[17]. According to the conducted experiment of the proposed method with an image resolution of size 224×224 , the recorded number of parameters are about 4.5M, which are less than the MobileNet V2, ESPNet V2 and COVID-Net as revealed in Table 7. It also shows that the proposed method has a higher image per second (IPS) processing rate, which is only slightly lower than than MobileNetV2, Table 7. Furthermore, Table 7 shows that the parameters of MobileNet v2 are 6.9M in size, with an image testing rate of 240 IPS, the size of the parameters of ESPNet v2 are 67M, while ShuffleNet V2 reaches 1.5M parameters with 57 IPS ,and SqueezeNet V2 reaches to 1.25M, with a testing time speed of 24 IPS.

6 | EXPERIMENTS

Python and Keras library backed with Tensorflow are used for all experiments. The experiments were conducted on an NVIDIA GTX-1080Ti GPU with a 12GB RAM Intel E5-2630 CPU processor. In the medical domain, the proposed LW-CovidNet is compared with five traditional models, that is, UNet[53], UNet-Attention[54], DeeplabV3[55], and MobileNet V2[46] as baseline methods

6.1 | Training

The division of the training images of datasets constitutes 80%(3616) for training, 20%(904) for validation. The dataset include Covid infected and normal images for the training. The

TABLE 3 Presenting the Five fold cross validation of the proposed method using Covid-19 dataset

Folds	AC	SN	SP	Precision	F1-Score
Fold1	98.2	95.3	98.8	98.0	95.7
Fold2	97.8	94.4	99.0	96.7	96.2
Fold3	97.5	96.8	99.1	96.8	95.4
Fold4	98.7	97.8	98.9	99.0	97.4
Fold5	98.8	95.7	99.2	97.7	98.1
Average	98.2	96.0	99.0	97.6	96.6

Network is trained at 200 epochs. The experiments on one GPU used batch sizes of 8,16,32. The images of covid, and normal images were included in the network's training process as a supervised learning. The five models were trained through the 5-fold cross-validation to extract an average from the results as shown in Table 3. In the network training, the binary cross entropy loss was used as a loss function.

$$L(\theta) = -\frac{1}{n} \sum_{i=1}^n [y_i \log(p_i) + (1 - y_i) \log(1 - p_i)]. \quad (4)$$

There are two classes, including infected and normal regions, in each input images in all experiments. y with a value of 1 denotes normal, and 0 denotes infected regions. The estimated probability of being infected or normal for the number of images is represented by $P(y)$. The learning rate of 0.001 was used for $L(\theta)$ in order to train the model. $L(\theta)$ was optimized by Adam optimizer, with three regularization parameters $\beta(1) = 0.9$, $\beta(2) = 0.999$ and AMSGrad= False.

6.2 | Performance metrics of evaluation

Accuracy(AC), sensitivity(SN) and specificity(SP) are fundamental detection metrics used by this study to calculate the effectiveness of proposed method. True Positives (TPs), False Negatives (FNs), False Positives (FPs) and True Negatives (TNs) are used to determine these metrics. True Positives (TPs) can be defined as the infected areas successfully identified by the model, whereas those classified as normal lie under False Negative (FN). Correspondingly, True Negative (TN) denotes the unaffected normal images that are correctly identified; if not, they fall under the False Positive (FP) category. The ability of LW-CovidNet to precisely spot an infected covid cases are known as sensitivity ($TP/(TP+FN)$). Similarly, the capability of LW-CovidNet to identify normal patients are known as its specificity ($TN/(FP+TN)$). Likewise, the proportion of correct detections can be used to define accuracy as $(TN+TP)/(TN+FP+FN+TP)$. The precision of the model in detecting an image as positive is assessed as $TP/(TP+FP)$. In addition, by taking the harmonic mean of a method's precision and sensitivity, the F1-Score integrates both into a single metric such as $F_1 = 2 \times \frac{\text{Precision} \times \text{SN}}{\text{Precision} + \text{SN}}$

TABLE 4 Comparing the quantifiable results of our method against other methods, evaluated on Covid dataset. All given values are in percentage. Numerical bold text indicates the best results

Model	Backbone	AC	SN	SP	AUC
UNet[53]	VGG16	86.05	85.4	93.18	96.6
UNet-Attention[54]	DenseNet161	93.1	91.0	90.8	94.9
Deeplab V3[55]	VGG16	96.09	98.5	95.09	90.3
MobileNet V2[46]	–	94.2	92.6	96.3	95.0
Proposed method	–	98.2	96.0	99.0	97.3

TABLE 5 Assessment of the Proposed Method Detection Results with State-of-the-Art methods, evaluated on Covid dataset. All given values are in percentage. Numerical bold text indicates the best results

Model	AC	SN	SP	Precision	F1-Score
Wang et al.[17]	94.0	92.5	94.8	90.9	91.6
Zhang et al.[56]	94.03	95.6	92.5	91.7	93.6
Horry et al.[25]	87.61	83.8	91.4	90.7	87.1
Ozkurt et al.[19]	94.80	94.9	94.7	87.8	91.2
Minaee et al.[23]	91.04	82.2	97.0	95.0	88.1
Apostolopouloset et al.[7]	97.35	98.9	96.1	95.0	96.9
Loey et al.[27]	89.16	76.0	98.1	96.5	85.0
Proposed method	98.2	96.0	99.0	97.6	96.6

6.3 | Results

In this work, it is determined that the novel composition of Standard and Depth-wise Separable convolutions with an Edge Attention Block can accurately detect covid-19 infected regions under various challenges such as similar spatial characteristics, multi-scale variations in texture and shapes and sizes of infected regions. The proposed method outperformed previous medical baseline methods such as UNet[53], UNet-Attention[54], DeeplabV3[55], and MobileNet V2[46] in terms of performance. The metrics-based evaluation of performance comparison with mentioned baseline methods are depicted in Table 4. According to this study, LW-CovidNet can effectively detect various pathogenic abnormalities due to its cost-effective nature, detection results of proposed method are depicted in Figure 7. It can be seen from Figure 7 that the proposed method can successfully detect boundaries of infected regions of covid-19 and also applies heatmaps to clearly visualize patient's X-ray reports to help expert for the better understanding of doctors in treatment and isolation process. Further, the proposed method is also qualitatively compared with other state-of-the-arts methods of Wang et al.[17], Horry et al.[25], Apostolopouloset et al.[7], Minaee et al.[23], Zhang et al.[56], Loey et al.[27], Ozkurt et al.[19]. Hence someone can clearly visualized from confusion metrics of Figure 9 and its corresponding Table 5 that the proposed method exceeds mentioned state-of-the-arts methods in realm of AC, SN, SP, Precision and F1-Score the

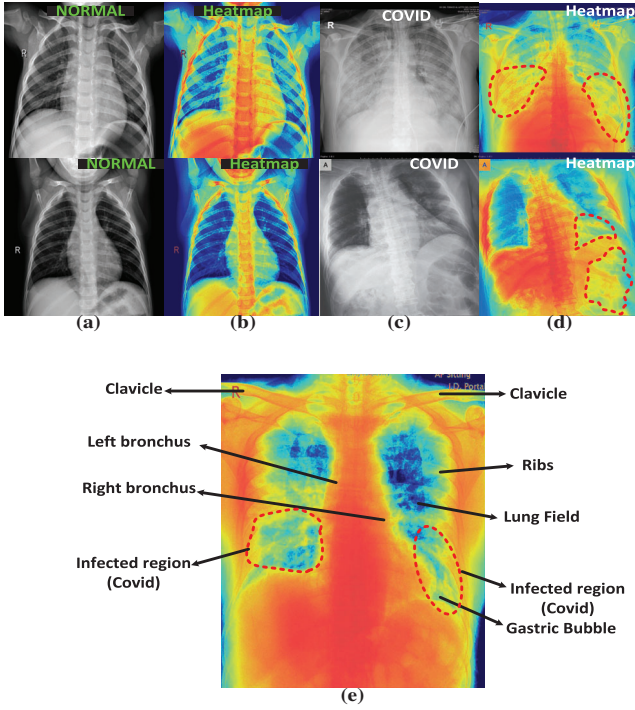


FIGURE 7 Covid and Normal cases can be easily distinguished by difference in color visualization: (a) and (b) visualization of normal images with heatmaps, (c) and (d) representing Covid-19 infected images with their corresponding heatmaps. (e) clear visualization of each regions of generated heatmap on resulting images. The model could be more beneficial for evaluating treatment efficacy based on the generated heatmap. It can also help doctors with patient diagnosis, follow-up, medication, and isolation

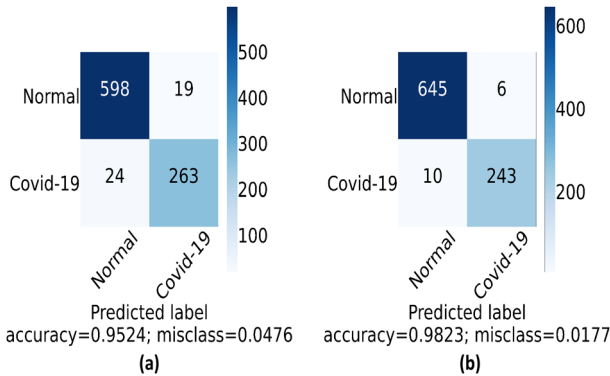


FIGURE 8 Confusion matrices on Covid-19 validation dataset: (a) Confusion matrix of LW-CovidNet using Standard convolutions; (b) Confusion matrix of LW-CovidNet using Standard convolutions with Depth-wise Separable convolutions

actual values in confusion metrics are shown by the vertical data, while the predicted values are represented by the horizontal data. The number of diagonal values in particular represents the accurate classification into covid-19 and normal cases. Moreover, it reveals from Figure 8 with corresponding Table 6, that utilization of Depth-wise Separable Convolutions with Standard Convolutions in proposed method increased the accuracy of model at margin of 3%, when compared with Standard

TABLE 6 Comparing the quantifiable results of our method using standard and standard with depth-wise separable convolutions, evaluated on Covid-19 dataset. SC is standard Conv and DSC is depth-wise separable conv

Method	AC	Precision	SN	F1-Score
LW-CovidNet- SC	95.24	93.2	92.0	93.0
LW-CovidNet-DSC	98.2	97.6	96.0	96.6

TABLE 7 Comparison with light weight models

Method	Layers	Image size	Parameters (M)	Speed (images per second)
MobileNet V2	28	224 × 224	6.9	240
ShuffleNet V2	44	224 × 224	1.5	57
SqueezeNet V2	18	224 × 224	1.25	24
ESPNet V2	–	224 × 224	67	–
COVID-Net	–	480 × 480	11.25	–
Ours	30	224 × 224	4.5	65

convolutions. Further, it can also realized from Table 6 that the proposed method exceeds other settings like only utilizing Standard convolutions in terms of AC, Precision, Sensitivity, and F1-Score at margin of 2.99%, 4.4%, 4%, and 3.7%, respectively. The proposed method is lightweight and computationally cost effective as compare to state-of-the-arts lightweight methods, as assessment with other popular methods are listed in Table 7. Moreover, Figure 10 depicts a receiver operating curve (ROC), which demonstrates the model's capacity to distinguish disease regions with incredible accuracy. A larger area under the curve indicates that the network is much more capable of disease recognition. The AUC of the LW-CovidNet, which is recorded as 97.3%, confirms proposed method's detection capacity. The capacity of LW-CovidNet to detect infected regions precisely is due to its ability to integrate Standard and Depth-wise separable convolutions, as well as the innovative methods of the increasing Receptive Field and Edge Attention Block.

6.4 | Ablation studies

We have conducted ablation studies to check the effectiveness of LW-CovidNet architecture with Edge-Attention block and other settings e.g different hyperparameters like b_α , b_β , b_{γ_1} , b_{γ_2} to demonstrate the efficacy of proposed method's various components. In ablation studies, we obtained more competitors by different hyperparameters settings like $S_1 = \text{LW-CovidNet+Max}$, $S_2 = \text{LW-CovidNet+Average}$, $S_3 = \text{LW-CovidNet+Average}$, $S_4 = \text{LW-CovidNet+Average}$ with varied b , $S_5 = \text{LW-CovidNet+ GAP}$, $S_6 = \text{LW-CovidNet+Edge Attention}$. The different hyperparameter settings of these competitors are shown in Table 8. In addition, we performed a statistical study using the mean of AC, SN, SP, values for

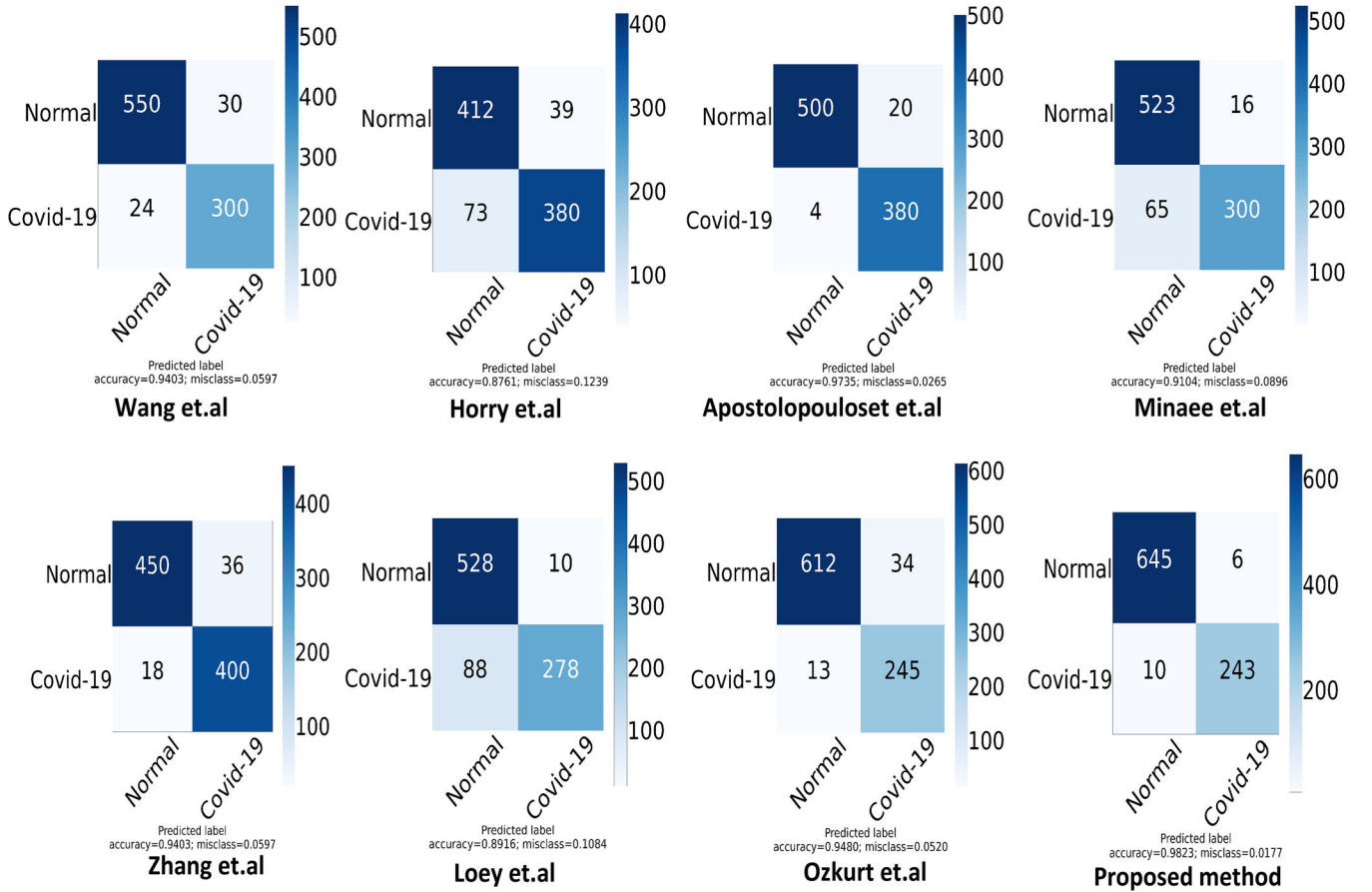


FIGURE 9 Comparison of proposed method with state-of-the-art methods using confusion metrics on Covid-19 dataset

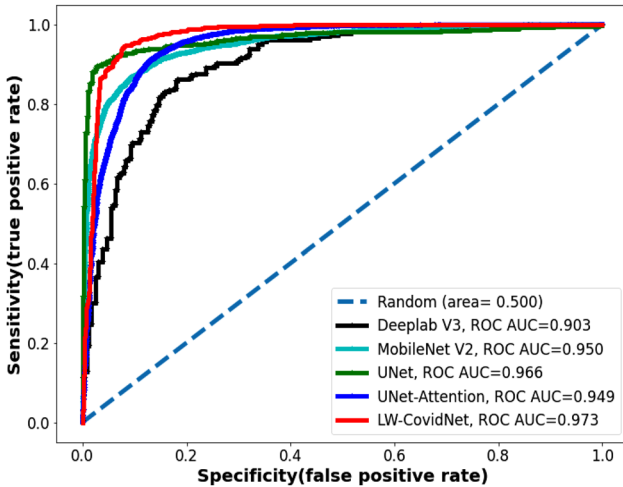


FIGURE 10 comparison of ROC curves to the current state-of-the-art baseline methods generated on the Covid validation dataset

various settings applied to covid-19 dataset as depicted in Table 9 with corresponding Figure 11 of ROC. Someone can clearly observe that LW-CovidNet with an Attention Block has superior results as compared to the other settings which can confirm the efficiency of the method. The proposed method

TABLE 8 Presenting the Ablation Study of proposed network in different settings

Methods	h_α	h_β	h_{γ_1}	h_{γ_2}
S_1	4	5	0.001	0.001
S_2	6	6	0.002	0.002
S_3	6	6	0.01	0.01
S_4	3	4	0.01	0.01
S_5	6	6	0.01	0.01
S_6	6	6	0.01	0.01

TABLE 9 Presenting the Ablation Study of qualitative assessment using detection metrics such as AC, SN, and SP with respect to Table 8. All given values are in percentage

Methods	AC	SN	SP	AUC
S_1	93.5	90.9	94.3	92.0
S_2	93.8	93.5	91.2	93.1
S_3	95.7	94.2	90.1	94.5
S_4	95.2	96.2	97.8	95.2
S_5	96.2	98.2	94.7	97.0
S_6	98.2	96.0	99.0	97.3

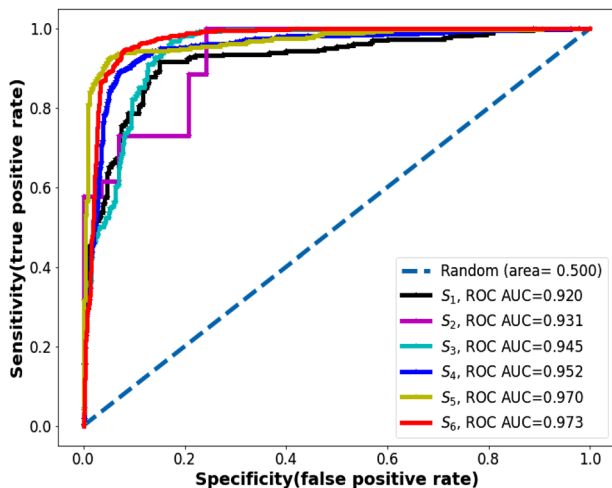


FIGURE 11 The ROC curves corresponding to the ablation study in different settings on Covid-19 validation set, with respect to Table 9

utilizes a hybrid method of integrating Standard and Depth-wise Separable convolutions with similar dilation rates and different kernel sizes, increased Receptive Field, also used an Edge Attention Block for better recognition of features, such methods can guide the network to overcome the detection challenges in presence of occlusions, such as similar spatial characteristics and irregular shapes of infected regions. Furthermore the attention method of proposed model is implemented with Global Average pooling with Relu and sigmoid, such settings are not sensitive to intra-class variations

It can clearly reveals from Tables 4–7 and Figures 8–11 that LW-CovidNet+Edge Attention method can achieves a good performance accuracy by setting $\gamma_1=L2(0.01)$, $\gamma_2=L2(0.01)$, $\alpha=6$, $\beta=6$, which indicates that the network hyperparameters should be weighted equally to ensure the finest balance of whole network with Edge Attention Block in guiding for the detection of infected regions based on covid-19.

7 | LIMITATIONS OF THE PROPOSED METHOD

This study, like any other neural network-based medical imaging studies, has significant limitations, such as visual region similarity and multi-scale differences in texture shape and size of infected regions, which lead to low disease detection performance in some circumstances. The model's performance may suffer as a result of the lack of training images available. Inadequate data makes it challenging to overcome the problem of class imbalance. This issue is addressed by an image augmentation technique that helps by synthesizing new images. However, the proposed method is compromised in case of discoloration in images, and it can function better by performing some well-explored pre-processing and post-processing methods. LW-CovidNet can be utilized in various disease detection processes such as Pneumonia and Tuberculosis detection. The future work will consider to explore the further competency of

the proposed method on multi-class disease detection and segmentation. Furthermore, in future study, More covid-19 sample images will be synthesized using the Generative Adversarial Network (GAN), which can be considered a data augmentation method to increase the detection performance.

8 | CONCLUSION

This study proposes a new method for detecting covid-19. The method combines Standard Convolutions with Depth-wise Separable convolutions increased Receptive Field through a new architecture design and also coupled an Edge Attention Block for accurate detection of infected regions from Chest X-ray images. The performance of this method is evaluated by simulations experiments carried over by combining four covid-19 datasets. The results have shown a significant improvement over other medical baselines methods such as MobileNet V2, Deeplab V3, UNet, and UNet-Attention and other current state-of-the-art methods based on transfer learning. This method revealed the efficacy in detection accuracy and other evaluation metrics with less number of network parameters and better processing speed as compare to state-of-the-arts methods such as MobileNet V2, ShuffleNet V2, SqueezeNet V2, ESPNet V2, COVID-Net.

ACKNOWLEDGEMENTS

The authors would like to express our gratitude to the anonymous reviewers for their helpful recommendations and informative comments. This work is partially supported by Shanghai Jiao Tong University (ZH2018ZDA25), the Science and Technology Commission of Shanghai Municipality Program (No. 18D1205903), National Natural Science Foundation of China (Nos. 61872242, 61472245).

CONFLICT OF INTEREST

The authors declare that they have no conflict of interest.

AUTHOR CONTRIBUTIONS

Noor Ahmed: Conceptualization, data curation, formal analysis, methodology, writing - original draft. Xin Tan: Writing - review and editing. Lizhuang Ma: Supervision.

DATA AVAILABILITY STATEMENT

Data will be available upon request.

ORCID

Noor Ahmed  <https://orcid.org/0000-0002-3745-0705>

REFERENCES

1. Bai, Y., Yao, L., Wei, T., Tian, F., Jin, D.Y., Chen, L., et al.: Presumed asymptomatic carrier transmission of covid-19. *Jama* 323(14), 1406–1407 (2020)
2. Chen, H., Guo, J., Wang, C., Luo, F., Yu, X., Zhang, W., et al.: Clinical characteristics and intrauterine vertical transmission potential of covid-19 infection in nine pregnant women: A retrospective review of medical records. *The Lancet* 395(10226), 809–815 (2020)

3. Long, C., Xu, H., Shen, Q., Zhang, X., Fan, B., Wang, C., et al.: Diagnosis of the coronavirus disease (covid-19): rrt-pcr or ct? *Eur. J. Radiol.* 126, 108961 (2020)
4. Kustin, T., Ling, G., Sharabi, S., Ram, D., Friedman, N., Zuckerman, N., et al.: A method to identify respiratory virus infections in clinical samples using next-generation sequencing. *Sci. Rep.* 9(1), 1–8 (2019)
5. Etienne, E.E., Nunna, B.B., Talukder, N., Wang, Y., Lee, E.S.: Covid-19 biomarkers and advanced sensing technologies for point-of-care (poc) diagnosis. *Bioengineering* 8(7), 98 (2021)
6. Alom, M.Z., Rahman, M., Nasrin, M.S., Taha, T.M., Asari, V.K.: Covid_mtnet: Covid-19 detection with multi-task deep learning approaches. *arXiv preprint arXiv:200403747* (2020)
7. Apostolopoulos, I.D., Mpesiana, T.A.: Covid-19: automatic detection from x-ray images utilizing transfer learning with convolutional neural networks. *Physical and Engineering Sciences in Medicine* 43(2), 635–640 (2020)
8. Horry, M.J., Chakraborty, S., Paul, M., Ulhaq, A., Pradhan, B., Saha, M., et al.: Covid-19 detection through transfer learning using multimodal imaging data. *IEEE Access* 8, 149808–149824 (2020)
9. Dutta, P., Roy, T., Anjum, N.: Covid-19 detection using transfer learning with convolutional neural network. In: 2021 2nd International Conference on Robotics, Electrical and Signal Processing Techniques (ICREST), pp. 429–432. IEEE, Piscataway (2021)
10. Sajid, N.: Covid-19 patients lungs x ray images 10000. <https://www.kaggle.com/nabeelsajid917/covid-19-x-ray-10000-images>. Accessed April 2020
11. Yang, X., He, X., Zhao, J., Zhang, Y., Zhang, S., Xie, P.: Covid-ct-dataset: a ct scan dataset about covid-19. *arXiv preprint arXiv:200313865* (2020)
12. Cohen, J.P., Morrison, P., Dao, L., Roth, K., Duong, T.Q., Ghassemi, M.: Covid-19 image data collection: Prospective predictions are the future. *arXiv preprint arXiv:200611988* (2020)
13. Chowdhury, M.E., Rahman, T., Khandakar, A., Mazhar, R., Kadir, M.A., Mahbub, Z.B., et al.: Can ai help in screening viral and covid-19 pneumonia? *IEEE Access* 8, 132665–132676 (2020)
14. Fan, D.P., Zhou, T., Ji, G.P., Zhou, Y., Chen, G., Fu, H., et al.: Inf-net: Automatic covid-19 lung infection segmentation from ct images. *IEEE Trans. Med. Imaging* 39(8), 2626–2637 (2020)
15. Shi, F., Wang, J., Shi, J., Wu, Z., Wang, Q., Tang, Z., et al.: Review of artificial intelligence techniques in imaging data acquisition, segmentation, and diagnosis for covid-19. *IEEE Rev. Biomed. Eng.* 14, 4–15 (2020)
16. Rajinikanth, V., Dey, N., Raj, A.N.J., Hassaniien, A.E., Santosh, K., Raja, N.: Harmony-search and otsu based system for coronavirus disease (covid-19) detection using lung ct scan images. *arXiv preprint arXiv:200403431* (2020)
17. Wang, L., Lin, Z.Q., Wong, A.: Covid-net: A tailored deep convolutional neural network design for detection of covid-19 cases from chest x-ray images. *Sci. Rep.* 10(1), 1–12 (2020)
18. Sarker, L., Islam, M.M., Hannan, T., Ahmed, Z.: Covid-densenet: A deep learning architecture to detect covid-19 from chest radiology images. (2020)
19. Ozturk, T., Talo, M., Yildirim, E.A., Baloglu, U.B., Yildirim, O., Acharya, U.R.: Automated detection of covid-19 cases using deep neural networks with x-ray images. *Comput. Biol. Med.* 121, 103792 (2020)
20. Bassi, P.R., Attux, R.: A deep convolutional neural network for covid-19 detection using chest x-rays. *Res. Biomed. Eng.* 1–10 (2021)
21. AlRakhami, M.S., Islam, M.M., Islam, M.Z., Asraf, A., Sodhro, A.H., Ding, W.: Diagnosis of covid-19 from x-rays using combined cnn-rnn architecture with transfer learning. *MedRxiv* 2020–08 (2021)
22. Mahmud, T., Rahman, M.A., Fattah, S.A.: Covxnet: A multi-dilation convolutional neural network for automatic covid-19 and other pneumonia detection from chest x-ray images with transferable multi-receptive feature optimization. *Comput. Biol. Med.* 122, 103869 (2020)
23. Minaee, S., Kafieh, R., Sonka, M., Yazdani, S., Soufi, G.J.: Deep-covid: Predicting covid-19 from chest x-ray images using deep transfer learning. *Med. Image Anal.* 65, 101794 (2020)
24. Rahimzadeh, M., Attar, A.: A modified deep convolutional neural network for detecting covid-19 and pneumonia from chest x-ray images based on the concatenation of xception and resnet50v2. *Inf. Med. Unlocked* 19, 100360 (2020)
25. Horry, M.J., Chakraborty, S., Paul, M., Ulhaq, A., Pradhan, B., Saha, M., et al.: X-ray image based covid-19 detection using pre-trained deep learning models. (2020)
26. Sethy, P.K., Behera, S.K.: Detection of coronavirus disease (covid-19) based on deep features. (2020)
27. Loey, M., Smarandache, F., M.Khalifa, N.E.: Within the lack of chest covid-19 x-ray dataset: a novel detection model based on gan and deep transfer learning. *Symmetry* 12(4), 651 (2020)
28. Bukhari, S.U.K., Bukhari, S.S.K., Syed, A., Shah, S.S.H.: The diagnostic evaluation of convolutional neural network (cnn) for the assessment of chest x-ray of patients infected with covid-19. *MedRxiv* (2020)
29. Raghu, M., Zhang, C., Kleinberg, J., Bengio, S.: Transfusion: Understanding transfer learning for medical imaging. *arXiv preprint arXiv:190207208* (2019)
30. LeCun, Y., Bottou, L., Bengio, Y., Haffner, P.: Gradient-based learning applied to document recognition. *Proc. IEEE* 86(11), 2278–2324 (1998)
31. Krizhevsky, A., Sutskever, I., Hinton, G.E.: Imagenet classification with deep convolutional neural networks. *Adv. Neural Inf. Process. Syst.* 25, 1097–1105 (2012)
32. Simonyan, K., Zisserman, A.: Very deep convolutional networks for large-scale image recognition. *arXiv preprint arXiv:14091556* (2014)
33. Huang, G., Liu, Z., Van.Der.Maaten, L., Weinberger, K.Q.: Densely connected convolutional networks. In: *Proceedings of the IEEE Conference on Computer Vision and Pattern Recognition*, pp. 4700–4708. IEEE, Piscataway (2017)
34. Larsson, G., Maire, M., Shakhnarovich, G.: Fractalnet: Ultra-deep neural networks without residuals. *arXiv preprint arXiv:160507648* (2016)
35. Szegedy, C., Liu, W., Jia, Y., Sermanet, P., Reed, S., Anguelov, D., et al.: Going deeper with convolutions. In: *Proceedings of the IEEE Conference on Computer Vision and Pattern Recognition*, pp. 1–9. IEEE, Piscataway (2015)
36. He, K., Zhang, X., Ren, S., Sun, J.: Deep residual learning for image recognition. In: *Proceedings of the IEEE Conference on Computer Vision and Pattern Recognition*, pp. 770–778. IEEE, Piscataway (2016)
37. Schmidhuber, J.: Deep learning in neural networks: An overview. *Neural Networks* 61, 85–117 (2015)
38. Jiang, X., Jin, Y., Yao, Y.: Low-dose ct lung images denoising based on multiscale parallel convolution neural network. *The Visual Comput.* 37(8), 2419–2431 (2021)
39. Luo, X., Tu, X., Ding, Y., Gao, G., Deng, M.: Expectation pooling: an effective and interpretable pooling method for predicting dna–protein binding. *Bioinformatics* 36(5), 1405–1412 (2020)
40. Wang, S.H., Tang, C., Sun, J., Yang, J., Huang, C., Phillips, P., et al.: Multiple sclerosis identification by 14-layer convolutional neural network with batch normalization, dropout, and stochastic pooling. *Front. Neurosci.* 12, 818 (2018)
41. Srivastava, N., Hinton, G., Krizhevsky, A., Sutskever, I., Salakhutdinov, R.: Dropout: A simple way to prevent neural networks from overfitting. *The Journal of Machine Learning Research* 15(1), 1929–1958 (2014)
42. Long, J., Shelhamer, E., Darrell, T.: Fully convolutional networks for semantic segmentation. In: *Proceedings of the IEEE Conference on Computer Vision and Pattern Recognition*, pp. 3431–3440. IEEE, Piscataway (2015)
43. Lin, M., Chen, Q., Yan, S.: Network in network. *arXiv preprint arXiv:13124400* (2013)
44. Qiu, S.: Global weighted average pooling bridges pixel-level localization and image-level classification. *arXiv preprint arXiv:180908264* (2018)
45. Ma, N., Zhang, X., Zheng, H.T., Sun, J.: Shufflenet v2: Practical guidelines for efficient cnn architecture design. In: *Proceedings of the European Conference on Computer Vision (ECCV)*, pp. 116–131. Springer, Berlin (2018)
46. Sandler, M., Howard, A., Zhu, M., Zhmoginov, A., Chen, L.C.: Mobilenetv2: Inverted residuals and linear bottlenecks. In: *Proceedings of the IEEE Conference on Computer Vision and Pattern Recognition*, pp. 4510–4520. IEEE, Piscataway (2018)
47. Howard, A.G., Zhu, M., Chen, B., Kalenichenko, D., Wang, W., Weyand, T., et al.: Mobilenets: Efficient convolutional neural networks for mobile vision applications. *arXiv preprint arXiv:170404861* (2017)

48. Zhang, X., Zhou, X., Lin, M., Sun, J.: Shufflenet: An extremely efficient convolutional neural network for mobile devices. In: Proceedings of the IEEE Conference on Computer Vision and Pattern Recognition, pp. 6848–6856. IEEE, Piscs (2018)
49. Bao, H.: Investigations of the influences of a cnn’s receptive field on segmentation of subnuclei of bilateral amygdalae. arXiv preprint arXiv:191102761 (2019)
50. Koutini, K., Eghbal.Zadeh, H., Dorfer, M., Widmer, G.: The receptive field as a regularizer in deep convolutional neural networks for acoustic scene classification. In: 2019 27th European Signal Processing Conference (EUSIPCO), pp. 1–5. IEEE, Piscataway (2019)
51. Mehta, S., Rastegari, M., Shapiro, L., Hajishirzi, H.: Espnetv2: A light-weight, power efficient, and general purpose convolutional neural network. In: Proceedings of the IEEE/CVF Conference on Computer Vision and Pattern Recognition, pp. 9190–9200. (2019)
52. Iandola, F.N., Han, S., Moskewicz, M.W., Ashraf, K., Dally, W.J., Keutzer, K.: Squeezenet: Alexnet-level accuracy with 50x fewer parameters and < 0.5 mb model size. arXiv preprint arXiv:160207360 (2016)
53. Ronneberger, O., Fischer, P., Brox, T.: U-net: Convolutional networks for biomedical image segmentation. In: International Conference on Medical image computing and computer-assisted intervention, pp. 234–241. Springer, (2015)
54. Oktay, O., Schlemper, J., Folgoc, L.L., Lee, M., Heinrich, M., Misawa, K., et al.: Attention u-net: Learning where to look for the pancreas. arXiv preprint arXiv:1804.03999 (2018)
55. Chen, L.C., Zhu, Y., Papandreou, G., Schroff, F., Adam, H.: Encoder-decoder with atrous separable convolution for semantic image segmentation. In: Proceedings of the European Conference on Computer Vision (ECCV), pp. 801–818. Springer, Berlin (2018)
56. Zhang, J., Xie, Y., Pang, G., Liao, Z., Verjans, J., Li, W., et al.: Viral pneumonia screening on chest x-rays using confidence-aware anomaly detection. IEEE Trans. Med. Imaging 40(3), 879–890 (2020)

How to cite this article: Ahmed, N., Tan, X., Ma, L.: LW-CovidNet: Automatic covid-19 lung infection detection from chest X-ray images. IET Image Process. , 1–13 (2022). <https://doi.org/10.1049/ipr2.12637>